Hindawi
Geofluids
Volume 2023, Article ID 4003656, 21 pages
https://doi.org/10.1155/2023/4003656

WILEY | Hindawi

Research Article

An Explicit Method for Estimating the Average Reservoir Pressure and Gas in Place Based on the Gas Property Polynomial Function

Lixia Zhang[1] **Hao Jiang,**[2] **Yong Li,**[1] **Xinmin Song,**[1] **and Yang Li**[3]

[1]*Research Institute of Petroleum Exploration and Development, PetroChina, Beijing 100083, China*
[2]*School of Petroleum Engineering, Southwest Petroleum University, Chengdu, Sichuan 610500, China*
[3]*The Fifth Oil Production Plant of PetroChina Changqing Oilfield Company, Xi'an, Shaanxi 710200, China*

Correspondence should be addressed to Lixia Zhang; zlx18101302186@126.com

Received 11 July 2022; Revised 7 October 2022; Accepted 14 October 2022; Published 30 January 2023

Academic Editor: Qianyou Wang

The fast and accurate determination of average reservoir pressure (ARP) and gas reserves is vital for the analysis and forecasting of gas well performance. An explicit and relatively rigorous method for estimating the ARP and gas in place, based on the dynamic material balance equation and the gas property polynomial function (GPPF), is presented to circumvent such drawbacks as high cost, empiricism, poor adaptability to variable production schedules, and the necessity for iteration processes, by which current approaches usually have been limited. The gas flow model is solved by introducing pseudofunctions and considering the compressibility effects of rock and irreducible water, and the pressure-rate correlations during boundary-dominated flow (BDF) which constitute the theoretical proofs of this method are derived from the superposition principle coupled with the constant rate solution. Production data under different production scenarios prove it effective. The error of estimation for formation pressure and gas reserves hardly ever goes beyond 4% given that the BDF condition is generally satisfied by the rate and bottom hole flowing pressure (BHP) data. We employ the GPPF to capture the nonlinear variations of gas viscosity and Z-factor, helpful to implement a quick conversion between pressure and pseudopressure and to solve the integral equation concerning pseudopressure and thus valid in overcoming the limitations of previous methods concerning pressure or pressure squared. The proposed methodology boasts its simpleness and practicability, which not only dispenses with iterations on pseudotime but also applies to various production systems of gas wells under constant BHP, constant rate, or variable BHP/variable rate conditions.

1. Introduction

The determination of ARP is an essential part of the analysis and prediction of well performance. Gas reservoir pressure data can be related to cumulative gas production through the static material balance equation (SMBE). Gas reserves can be estimated directly by that relationship if pressures are obtained by multiple measurements which are unfortunately time-consuming and have a high cost. The ARP profile in turn can also be determined by the SMBE when reserves are available.

Generally, the ARP is extrapolated by the pressure transient analysis (PTA) [1–4], including the methods proposed by Horner [5], Miller et al. [6], Matthews et al. [7], Dietz [8], Ramey and Cobb [9], and Odeh and Al-Hussainy [10]. Formation pressure can also be estimated by empirical exponential [11] or binomial [12, 13] productivity equations using systematic well test (flow-after-flow test) data and can be measured directly after shutting in the well. These methods, however, are not suitable to be used frequently due to their high cost, which brings difficulties in continuous pressure estimation. Researchers, hence, began to explore cheaper methods for production data analysis (PDA).

PDA involves the estimation of reservoir information through theoretical or empirical models by using daily measurement data such as rate, pressure, and cumulative production. The rate transient analysis (RTA), receiving wide attention due to its economical and practical characteristics, is an important type of PDA. The research on the RTA can be traced back to the production decline analysis by Arps

[14] using statistics. The reported method is simple and applies to constant BHP production systems, but it was not proved theoretically at that time.

Fetkovich [15, 16] first introduced the idea of PTA into RTA. He incorporated the constant BHP analytical solution of the unsteady flow and Arps' curves into the log-log plots and performed the production decline analysis by a type curve fitting similar to PTA. Fetkovich proved theoretically that the relationship between the dimensionless rate q_{dD} and the dimensionless time t_{dD} for constant pressure systems follows the exponential decline law in late BDF, which, as a representative of RTA, overcomes the drawback (empiricism) of Arps' curves. However, Fetkovich curves can only be applied to the constant pressure production systems of slightly compressible fluids for ignoring the changes in fluid properties.

To consider the variations of gas properties during depletion, Carter [17, 18] introduced the variable, $\lambda = \mu_{\mathrm{i}} C_{\mathrm{gi}} /(\mu C_{\mathrm{g}})$, to explain changes in viscosity and compressibility, and presented Carter curves to analyze the gas well data. The pressure drop parameter, λ, nevertheless, is an average from BHP p_{wf} to the original reservoir pressure p_{i} and does not change with the ARP. Therefore, it is only an approximate method for analyzing gas well data under the constant BHP condition.

To tackle fluctuations in production schedules and changes in gas properties, pseudopressure and pseudotime functions were introduced by Blasingame and Lee [19], and he proposed, based on the pressure-rate relation in BDF and SMBE for constant volume gas reservoirs, a method for iterative calculation of reserves and pseudotime, where the ARP can be estimated by the SMBE.

The material balance pseudotime function t_{ca} can greatly eliminate the influence of production fluctuations on the analysis, but its determination requires iterations since the ARP is implicit. Blasingame et al. [20] proposed the concept of constant BHP equivalent time function. One can use the constant BHP solution to analyze data under variable BHP/variable rate conditions. Its innovation is the conversion from the constant rate analog time (t_{ca}) into the constant pressure analog time function; nonetheless, for gas wells, determining the parameters, m_{bdf} and b, still requires iterations on t_{ca}.

Palacio and Blasingame [21], based on the previous BDF pressure-rate correlation [19], proved that the relationship between q_{dD} and t_{dD} defined by the pseudopressure and t_{ca} is always consistent with the harmonic decline, thus developing a type curve analysis method that can explain variable rate/variable pressure data. As another representative of RTA, Blasingame's type curves boast the ability to explain the changes in production schedules and fluid properties during BDF.

In addition, other type curve analysis methods such as Agarwal-Gardner curves [22, 23] and normalized pressure integral (NPI) curves [24] actually change the drawing functions, while their analysis principles are basically the same.

Aiming at constant rate gas wells in volumetric gas reservoirs, Mattar and McNeil [25, 26] proposed the flowing material balance (FMB) method for estimating reserves by using the ratio p/Z at the BHP to replace the value at the ARP. In fact, the slope of the straight line plotted by p/Z and the cumulative gas production when the reference pressure is the BHP is not equal to the result at ARP. Later, some researchers [27, 28] improved it, but their approaches still could not meet the requirements for analyzing variable rate/variable BHP data.

To deal with fluctuations in flow rate, Mattar and Anderson [29, 30] improved the previous FMB, based on the "stabilized flow" solution and the SMBE, and developed the dynamic material balance (DMB) method (or variable rate FMB), which considers changes in property parameters and production scenarios. In terms of theory, it is more rigorous but requires iterations on the ARP and t_{ca}.

Those methods for determining the ARP or reserves are usually implicit since t_{ca} needs to be evaluated iteratively at the ARP when one analyzes gas production data using the classical PDA/RTA methods.

Later, some researchers began to explore explicit methods. The research of Ye and Ayala [31] is quite representative. They ignored the viscosity term in the pseudopressure and introduced gas density (ρ) and pseudotime factor (β) to describe the gas flow. The dimensionless boundary, r_{eD}, is determined by the solution characterizing the liquid flow due to its small deviation away from the solution of gas flow in the early stage when gas property changes are small, while the values of λ, i.e., $\mu_{\mathrm{i}} C_{\mathrm{gi}}/(\mu C_{\mathrm{g}})$, and β are estimated by the large deviation between the two solutions during BDF. Gas reserves are determined by the approximate relation between λ and ρ. This work assumes a constant straight-line slope in the $\mu \cdot C_{\mathrm{g}}$ vs. ρ logarithmic curve, and it is mainly targeted at the constant pressure production systems.

Stumpf and Ayala [32] explained the physical connotations of the Arps' hyperbolic-decline model for constant BHP gas wells and proposed a method for determining reserves using the rate vs. cumulative production data in early BDF (the hyperbolic window). It is necessary to identify the start/end moments of the hyperbolic window through curve fitting and determine the integral average of the decline exponent, which is cumbersome and only applicable to constant BHP conditions.

Zhang et al. [33] presented an approach to determine reserves without pseudotime iterations by combining the material balance condition derived from the SMBE with the pseudopressure approximation condition derived from the DMB equation.

Following Stumpf and Ayala's research [32], Wang and Ayala [34] extended the hyperbolic decline model by postulating a constant ratio of the pseudo-BHP to the pseudo-ARP and determined reserves by using curve fitting and linear analysis of the rate vs. cumulative production curve. Both Stumpf and Wang used the integral mean from the pseudo-BHP to the pseudo-ARP when calculating the decline exponent, but it is actually a function of ARP. It seems more reasonable that the integration range is evaluated by the variation range of ARP during the target period.

Jongkittinarukorn et al. [35] also discussed the changes in decline rate and decline exponent for constant BHP gas wells in volumetric reservoirs. They explained the relationship between production rate, decline rate, decline exponent, and λ vs. $(p/Z)/(p_i/Z_i)$ based on the stabilized flow equation developed by Ansah et al. [36, 37] and estimated gas reserves by that explanation. The workflow, which infers the decline rate profile by the rate-time profile and then determines the decline exponent profile, however, may cause undesirable results.

In conclusion, currently available PDA methods for determining gas reservoir pressure and reserves mainly include type curve analysis [38, 39], FMB [25–28], pseudotime iteration methods (such as variable rate reservoir limits testing developed by Blasingame and Lee [19] and DMB developed by Mattar and Anderson [29, 30]), and various explicit methods. Among them, Carter's type curves are limited to constant pressure conditions. Furthermore, variable rate reservoir limits testing, DMB, and Blasingame's type curves can dispose fluctuations in production conditions, but the pseudotime needs to be calculated iteratively. The modified FMB approach is only suitable for constant rate gas wells, while explicit methods that rely on traditional decline parameters can merely handle constant BHP conditions or specific pressure conditions [32, 34, 35]. In addition, most of these methods do not consider the compressibility of pores and irreducible water during pressure depletion.

Therefore, based on the DMB equation and the gas property polynomial function (GPPF), this research is aimed at developing an explicit method for estimating the ARP and gas in place under variable BHP/variable rate conditions, which also captures the similar superiority of implicit techniques and considers the compressibility effects.

2. Model Development

The developed methodology here is based on the pressure-rate relationships during BDF (especially the dynamic material balance equation, DMBE) for a gas well in a bounded reservoir and the gas property polynomial function for pseudopressure approximation. This paper takes the radial reservoir system as an example to derive the DMBE also applicable to noncircular boundary reservoirs. The theoretical bases of the proposed method for the determination of ARP and gas reserves will be demonstrated below.

2.1. Pressure-Rate Correlations in BDF. The gas flow through porous media conforms to Darcy's law, namely,

$$\vec{v}_{\mathrm{g}} = -\frac{K}{\mu}\nabla p. \tag{1}$$

The state equations of rock [40, 41] are represented by

$$\phi = \phi_{\mathrm{i}} \cdot e^{C_\phi (p-p_{\mathrm{i}})}, \tag{2}$$

$$V_{\mathrm{p}} = V_{\mathrm{pi}} \cdot e^{C_\phi (p-p_{\mathrm{i}})}. \tag{3}$$

The state equations of irreducible water can be written as

$$V_{\mathrm{w}} = V_{\mathrm{wi}} \cdot e^{-C_{\mathrm{w}} (p-p_{\mathrm{i}})}, \tag{4}$$

$$S_{\mathrm{wc}} = \frac{V_{\mathrm{w}}}{V_{\mathrm{p}}} = S_{\mathrm{wci}} \cdot e^{-\left(C_{\mathrm{w}}+C_\phi\right)(p-p_{\mathrm{i}})}. \tag{5}$$

The state of gas is mainly characterized by its density function and gas compressibility:

$$\rho_{\mathrm{g}} = \frac{pM}{ZRT}, \tag{6}$$

$$C_{\mathrm{g}} = \frac{ZT}{p} \cdot \frac{d}{dp}\left(\frac{p}{ZT}\right) \approx \frac{Z}{p} \cdot \frac{d}{dp}\left(\frac{p}{Z}\right). \tag{7}$$

The mass conservation equation of gas can be obtained by the combination of the motion equation and the state equations, i.e.,

$$-\nabla \cdot \left(\rho_{\mathrm{g}} \vec{v}_{\mathrm{g}}\right) + \dot{q}_{\mathrm{g}} = (1 - S_{\mathrm{wc}})\frac{\partial\left(\rho_{\mathrm{g}}\phi\right)}{\partial t} + \rho_{\mathrm{g}}\phi\frac{\partial(1 - S_{\mathrm{wc}})}{\partial t}. \tag{8}$$

Substituting Equations (1)–(7) into Equation (8), the governing equation of gas flow in the porous media can be expressed as

$$\nabla \cdot \left(\frac{p}{\mu Z}\nabla p\right) = \frac{\phi_{\mathrm{i}}\mu_{\mathrm{i}}C_{\mathrm{ti}}}{K} \cdot \frac{\mu C_{\mathrm{t}}}{\mu_{\mathrm{i}}C_{\mathrm{ti}}} \cdot \frac{p}{\mu Z}\frac{\partial p}{\partial t}, \tag{9}$$

$$C_{\mathrm{t}} = e^{C_\phi (p-p_{\mathrm{i}})}\left[(1 - S_{\mathrm{wc}})C_{\mathrm{g}} + C_\phi + S_{\mathrm{wc}}C_{\mathrm{w}}\right]. \tag{10}$$

It is difficult to directly solve the nonlinear differential equation, Equation (9), because the gas viscosity, the deviation factor, and the gas compressibility are all functions of pressure and temperature. Even if under the isothermal condition, they all change with pressure. Hence, the pseudofunctions of real time and real pressure are introduced:

$$t_{\mathrm{a}} = \mu_{\mathrm{i}}C_{\mathrm{ti}}\int_0^t \frac{1}{\mu C_{\mathrm{t}}}dt, \tag{11}$$

$$p_p = p_{\mathrm{i}} + \frac{\mu_{\mathrm{i}}Z_{\mathrm{i}}}{p_{\mathrm{i}}}\int_{p_{\mathrm{i}}}^{p} \frac{\xi}{\mu(\xi)Z(\xi)}d\xi. \tag{12}$$

By substituting Equations (11) and (12) into Equation (9), one obtains

$$\nabla^2 p_p = \frac{\phi_{\mathrm{i}}\mu_{\mathrm{i}}C_{\mathrm{ti}}}{K} \cdot \frac{\partial p_p}{\partial t_{\mathrm{a}}}. \tag{13}$$

To simplify the calculation of the integral term in the pseudopressure in the field practice, the integrand $f(p)$ in the two cases of high pressure and low pressure is often approximated as follows, respectively:

$$f(p)=\frac{p}{\mu(p)Z(p)}\approx\begin{cases}\dfrac{p}{C_0}\ (p<13.8\,\mathrm{MPa}),\\[2mm]\dfrac{1}{C_1}\ (p>20.7\,\mathrm{MPa}),\end{cases}$$

$$F(p)=\int\frac{p}{\mu(p)Z(p)}dp=\begin{cases}\dfrac{1}{2C_0}p^2+C_0{}'\ (p<13.8\,\mathrm{MPa}),\\[2mm]\dfrac{1}{C_1}p+C_1{}'\ (p>20.7\,\mathrm{MPa}).\end{cases}\tag{14}$$

It should be noted that this approach of using pressure or pressure squared to approximate pseudopressure is difficult to capture the pressure drop process that spans two pressure ranges and may cause large errors. Therefore, the mathematical model of gas flow in a circular bounded reservoir under the constant production rate condition is given in the rigorous form of pseudopressure (in the international system of units, $\alpha_t=1$, $\alpha_p=2\pi$):

$$\begin{gathered}\frac{\partial^2 p_p}{\partial r^2}+\frac{1}{r}\cdot\frac{\partial p_p}{\partial r}=\frac{\phi_i\mu_i C_{ti}}{\alpha_t K}\cdot\frac{\partial p_p}{\partial t_a},\\ \left(r\frac{\partial p_p}{\partial r}\right)\bigg|_{r=r_w}=\frac{q\mu_i B_{gi}}{\alpha_p Kh},\\ \frac{\partial p_p}{\partial r}\bigg|_{r=r_e}=0,\quad p_p\big|_{t_a=0}=p_p(p_i).\end{gathered}\tag{15}$$

By solving nondimensionalized Equation (15), the dimensionless pressure-time relationship is given by

$$\begin{aligned}p_D=&\frac{2t_D}{r_{eD}{}^2-1}-\frac{r_{eD}{}^2}{r_{eD}{}^2-1}\ln r_D\\&+\frac{4r_{eD}{}^4\ln r_{eD}-3r_{eD}{}^4+2r_D{}^2\left(r_{eD}{}^2-1\right)+2r_{eD}{}^2+1}{4\left(r_{eD}{}^2-1\right)^2}\\&-\pi\sum_{n=1}^{\infty}\frac{e^{-\lambda_n{}^2\cdot t_D}\cdot J_1{}^2(r_{eD}\lambda_n)\left[Y_1(\lambda_n)J_0(r_D\lambda_n)-J_1(\lambda_n)Y_0(r_D\lambda_n)\right]}{\lambda_n\cdot\left[J_1{}^2(r_{eD}\lambda_n)-J_1{}^2(\lambda_n)\right]},\end{aligned}\tag{16}$$

$$r_D=\frac{r}{r_w},\tag{17}$$

$$t_D=\frac{\alpha_t K}{\phi_i\mu_i C_{ti}\cdot r_w{}^2}t_a,\tag{18}$$

$$p_D=\frac{\alpha_p Kh\left(p_{p_i}-p_p\right)}{q\mu_i B_{gi}}.\tag{19}$$

According to the superposition principle, pseudopressure drop caused by production fluctuations can be written as

$$p_{p_i}-p_p(r,t_a)=\sum_{i=1}^{m}\frac{\mu_i B_{gi}}{\alpha_p Kh}\cdot(q_i-q_{i-1})\cdot p_D(t_a-t_{a,i-1}).\tag{20}$$

Substituting Equation (16) into Equation (20), we obtain

$$\frac{p_{p_i}-p_{p_{wf}}}{q}=m_{bdf}\cdot t_{ca}+b,\tag{21}$$

$$m_{bdf}=\frac{2\pi\alpha_t}{\alpha_p}\cdot\frac{B_{gi}}{Ah\phi_i C_{ti}},\tag{22}$$

$$t_{ca}=\frac{\mu_i C_{ti}}{q(t)}\int_0^t\frac{q(t)}{\mu(p_{ave})C_t(p_{ave})}dt,\tag{23}$$

$$\begin{aligned}b=\frac{\mu_i B_{gi}}{\alpha_p Kh}\Bigg\{&\frac{4r_{eD}{}^4\ln r_{eD}-3r_{eD}{}^4+4r_{eD}{}^2-1}{4\left(r_{eD}{}^2-1\right)^2}\\&+\sum_{i=1}^{m}\frac{q_i-q_{i-1}}{q_m}\left[\sum_{n=1}^{\infty}\frac{2}{\lambda_n{}^2}\cdot l(t_a,\lambda_n)\right]\Bigg\},\end{aligned}\tag{24}$$

$$l(t_a,\lambda_n)=\frac{e^{-\left(\lambda_n{}^2\cdot\left(\alpha_t K/\phi_i\mu_i C_{ti}r_w{}^2\right)(t_a-t_{a,i-1})\right)}J_1{}^2(r_{eD}\lambda_n)}{J_1{}^2(r_{eD}\lambda_n)-J_1{}^2(\lambda_n)}.\tag{25}$$

Equation (21) reveals the relationship between BHP, production rate, and material-balance pseudotime where t_{ca} is the reference value under the ARP. The average pseudopressure of the gas reservoir is defined as

$$\left(p_p\right)_{ave}=\frac{1}{\pi(r_e{}^2-r_w{}^2)}\int_{r_w}^{r_e}p_p\cdot 2\pi r\cdot dr.\tag{26}$$

Differentiating Equation (20) with respect to pseudotime t_a and combining it with Equation (15), we can get

$$\begin{aligned}p_p-p_{p_{wf}}=&\frac{q_m\mu_i B_{gi}}{\alpha_p Kh(r_e{}^2-r_w{}^2)}\left(r_e{}^2\ln\frac{r}{r_w}-\frac{r^2-r_w{}^2}{2}\right)\\&-\frac{\mu_i B_{gi}}{\alpha_p Kh}\times\sum_{i=1}^{m}(q_i-q_{i-1})\Bigg\{\sum_{n=1}^{\infty}l(t_a,\lambda_n)\\&\cdot\left[-\frac{\pi}{\lambda_n}Y_1(\lambda_n)J_0\left(\frac{\lambda_n}{r_w}r\right)\right.\\&\left.+\frac{\pi}{\lambda_n}J_1(\lambda_n)Y_0\left(\frac{\lambda_n}{r_w}r\right)-\frac{2}{\lambda_n{}^2}\right]\Bigg\}.\end{aligned}\tag{27}$$

Substituting Equation (27) into Equation (26) gives

$$\begin{aligned}\left(p_p\right)_{ave}=&p_{p_{wf}}+\frac{q_m\mu_i B_{gi}}{\alpha_p Kh}\cdot\frac{4r_{eD}{}^2+4r_{eD}{}^4\ln r_{eD}-3r_{eD}{}^4-1}{4\left(r_{eD}{}^2-1\right)^2}\\&+\frac{\mu_i B_{gi}}{\alpha_p Kh}\sum_{i=1}^{m}(q_i-q_{i-1})\left[\sum_{n=1}^{\infty}l(t_a,\lambda_n)\cdot\frac{2}{\lambda_n{}^2}\right].\end{aligned}\tag{28}$$

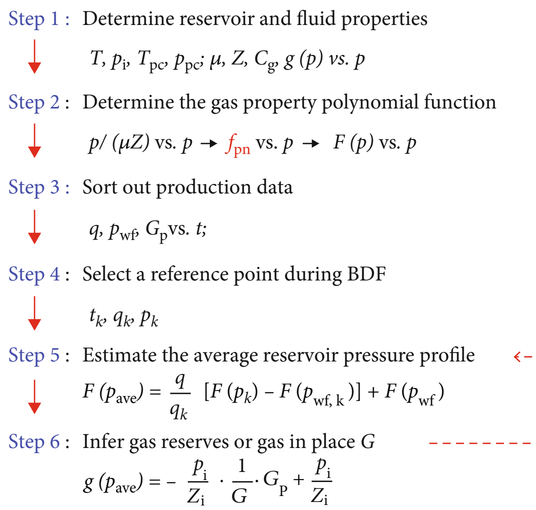

Figure 1: The workflow for estimation of ARP and reserves.

By applying $p_p(p_{\text{ave}}) = p_{p_{\text{ave}}} \approx (p_p)_{\text{ave}}$, Equation (28) can be rewritten as

$$p_{p_{\text{ave}}} = p_{p_{\text{wf}}} + q \cdot b. \tag{29}$$

Equation (29), termed "dynamic material balance equation" (DMBE), reveals the internal relationship between the ARP, BHP, and production rate. The value of b in Equations (21) and (29) changes very slowly with time in the BDF stage and can be approximated to a certain constant during the evaluation period; that is to say, the "boundary dominated flow condition" holds.

2.2. Determination of ARP. According to the definition of pseudopressure Equation (12), one can rewrite Equation (29) as

$$q = \frac{p_{p_{\text{ave}}} - p_{p_{\text{wf}}}}{b} = \frac{1}{b} \cdot \frac{\mu_{\text{i}} Z_{\text{i}}}{p_{\text{i}}} \left[\int_{p_{\text{i}}}^{p_{\text{ave}}} f(\xi) d\xi - \int_{p_{\text{i}}}^{p_{\text{wf}}} f(\xi) d\xi \right]. \tag{30}$$

Knowing the average formation pressure (p_k) at some time (t_k), we have

$$q_k = \frac{1}{b} \cdot \frac{\mu_{\text{i}} Z_{\text{i}}}{p_{\text{i}}} \int_{p_{\text{wf},k}}^{p_k} f(\xi) d\xi. \tag{31}$$

From Equations (30) and (31), it follows

$$\int_{p_{\text{wf}}}^{p_{\text{ave}}} f(\xi) d\xi = \frac{q}{q_k} \int_{p_{\text{wf},k}}^{p_k} f(\xi) d\xi. \tag{32}$$

Equation (32) is an integral equation derived from the DMBE. According to the reservoir pressure at a certain moment in the BDF stage and the recorded production data of the gas well (such as production rate and BHP), the reservoir pressure at each moment can be inferred by solving Equation (32). Directly using the pressure or pressure square method described above to solve it may cause large errors, while using numerical integration (such as the Romberg algorithm) may be time-consuming. Hence, this paper uses a polynomial to approximate the integrand f, namely,

Table 1: Property parameters for numerical simulations.

Property parameters	Property values
ϕ_{i}	0.190
K_r	8 mD
K_θ	8 mD
K_z	0.800 mD
S_{wci}	0.210
h	8 m
dr	1.500 m
$d\theta$	3°
dz	8 m
p_{i}	60 MPa
T_{i}	373.150 K
T_{sc}	293.150 K
p_{sc}	1.013×10^5 Pa
T_{pc}	205.760 K
p_{pc}	4.590 MPa
r_{e}	450 m
r_{w}	0.100 m
ρ_{sc}	0.778 kg/m^3
M	18.660 g/mol
Z_{sc}	0.997
Z_{i}	1.307
C_ϕ	5.335×10^{-4} MPa^{-1}
C_{w}	4.002×10^{-4} MPa^{-1}
μ_{w}	0.289 cp
μ_{i}	3.434×10^{-2} cp
μ_{sc}	1.064×10^{-2} cp
C_{gi}	7.230×10^{-3} MPa^{-1}
C_{ti}	6.329×10^{-3} MPa^{-1}
B_{gi}	2.817×10^{-3} m^3/m^3
G	271 300 553 m^3

$$f(p) = \frac{p}{\mu(p)Z(p)} \approx f_{\text{pn}}(p) = c_6 p^6 + c_5 p^5 + c_4 p^4 + c_3 p^3 + c_2 p^2 + c_1 p + c_0. \tag{33}$$

So, the original function of $f(p)$ can be expressed as

$$F(p) = \int \frac{p}{\mu(p)Z(p)} dp \approx \frac{c_6}{7} p^7 + \frac{c_5}{6} p^6 + \frac{c_4}{5} p^5 + \frac{c_3}{4} p^4 + \frac{c_2}{3} p^3 + \frac{c_1}{2} p^2 + c_0 p + C. \tag{34}$$

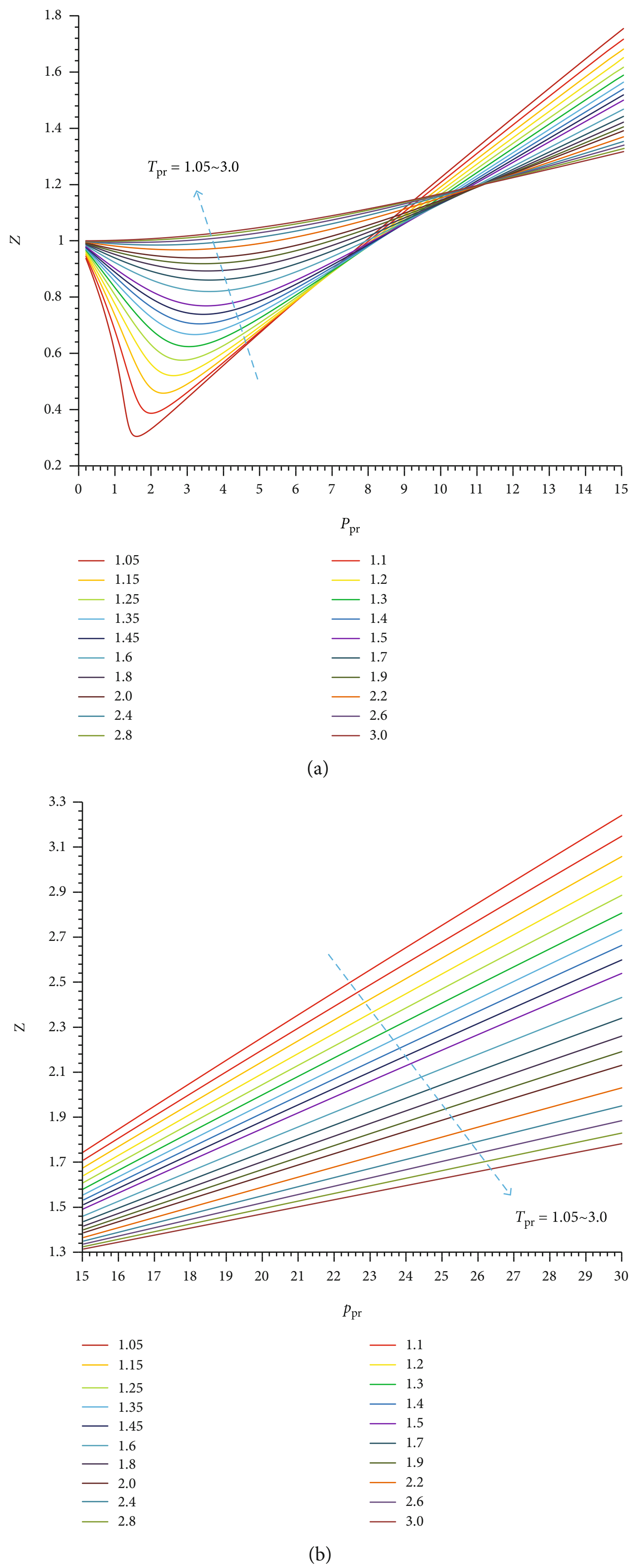

Figure 2: (a) Compressibility factors (Z-factors) of natural gases obtained by the Hall-Yarborough correlations at pseudoreduced pressures of 0.2 to 15. (b) Compressibility factors (Z-factors) of natural gases obtained by the Hall-Yarborough correlations at pseudoreduced pressures of 15 to 30.

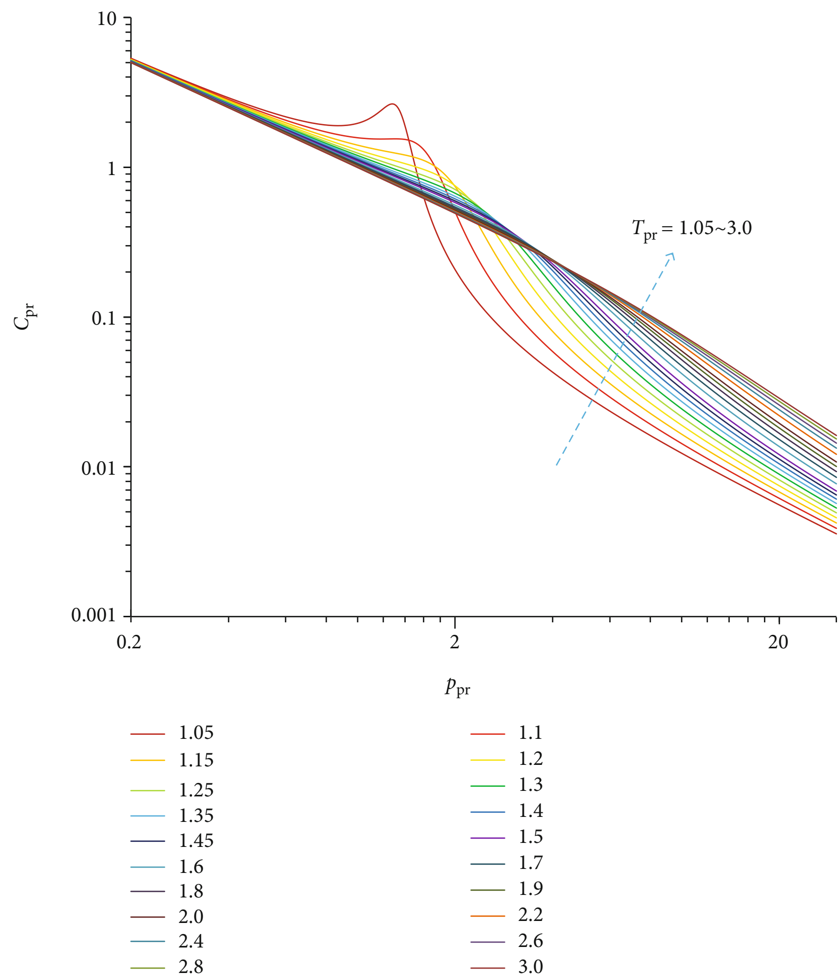

Figure 3: Pseudoreduced compressibility (C_{pr}) of natural gases obtained by the Hall-Yarborough correlations at pseudoreduced pressures of 0.2 to 30.

For convenience, the arbitrary constant C is taken to be zero in the paper. Equation (32) can be expressed analytically as

$$F(p_{ave}) = \frac{q}{q_k}\left[F(p_k) - F\left(p_{wf,k}\right)\right] + F(p_{wf}). \tag{35}$$

The left term of Equation (35), $F(p_{ave})$, is the polynomial function dependent on gas properties. Knowledge of the right term of Equation (35) can solve the values of p_{ave} in the interval of (p_{wf}, p_i) by the polynomial rooting, bisection, or Newton iteration method.

2.3. Estimation of Gas Reserves. The material balance for a bounded gas reservoir involves the elastic expansion of natural gas, the shrinkage of pores, and the expansion of irreducible water. The three elastic energy supplies the output of natural gas, namely,

$$\left(GB_g - GB_{gi}\right) + \Delta V_p + \Delta V_w = G_p B_g. \tag{36}$$

The gas volume factor, B_{gi} and $B_g(p_{ave})$, can be expressed as

$$\begin{aligned} B_{gi} &= \frac{Z_i T_i}{p_i} \cdot \frac{p_{sc}}{Z_{sc} T_{sc}}, \\ B_g(p_{ave}) &= \frac{ZT}{p_{ave}} \cdot \frac{p_{sc}}{Z_{sc} T_{sc}}. \end{aligned} \tag{37}$$

The volume of irreducible water and rock pores under original formation conditions can be written as

$$\begin{aligned} V_{wi} &= \frac{GB_{gi}}{1 - S_{wci}} S_{wci}, \\ V_{pi} &= \frac{GB_{gi}}{1 - S_{wci}}. \end{aligned} \tag{38}$$

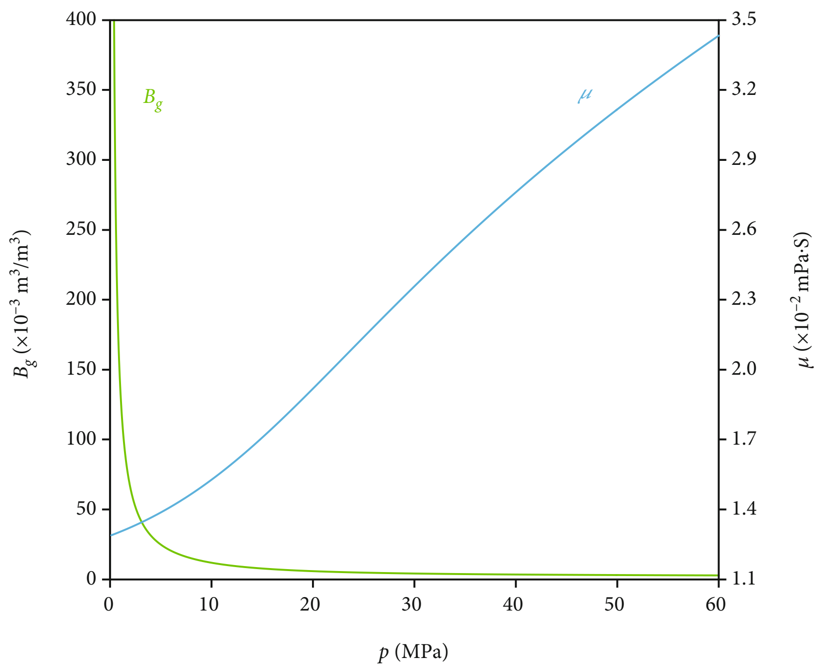

FIGURE 4: Gas formation volume factor (B_g) and gas viscosity (μ) vs. pressure (p) for case studies.

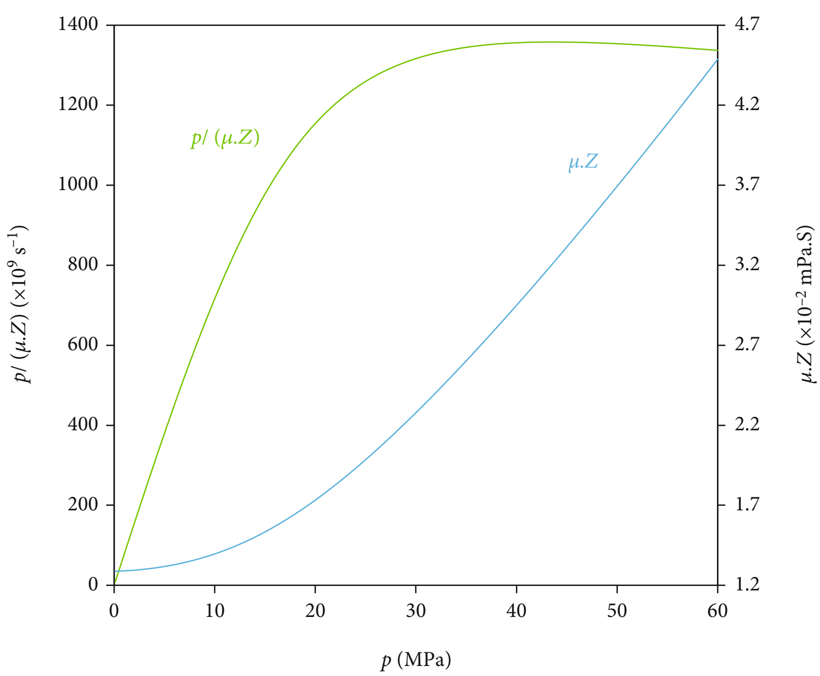

FIGURE 5: $p/(\mu Z)$ and μZ vs. pressure (p) for case studies.

It is reasonably assumed that the gas reservoir temperature remains unchanged during gas production. Substituting Equations (3), (4), (37), and (38) into Equation (36) yields

$$\frac{p_{\mathrm{ave}}}{Z(p_{\mathrm{ave}})} \cdot \frac{e^{C_\phi (p_{\mathrm{ave}}-p_{\mathrm{i}})} - S_{\mathrm{wci}} e^{-C_{\mathrm{w}}(p_{\mathrm{ave}}-p_{\mathrm{i}})}}{1 - S_{\mathrm{wci}}} = \frac{p_{\mathrm{i}}}{Z_{\mathrm{i}}}\left(1 - \frac{G_{\mathrm{p}}}{G}\right). \quad (39)$$

For expression convenience, an elastic effect function g related to pressure and compressibilities (of the rock and irreducible water) is introduced as follows:

$$g(p) = \frac{p}{Z(p)} \cdot \frac{e^{C_\phi (p-p_{\mathrm{i}})} - S_{\mathrm{wci}} e^{-C_{\mathrm{w}}(p-p_{\mathrm{i}})}}{1 - S_{\mathrm{wci}}}. \quad (40)$$

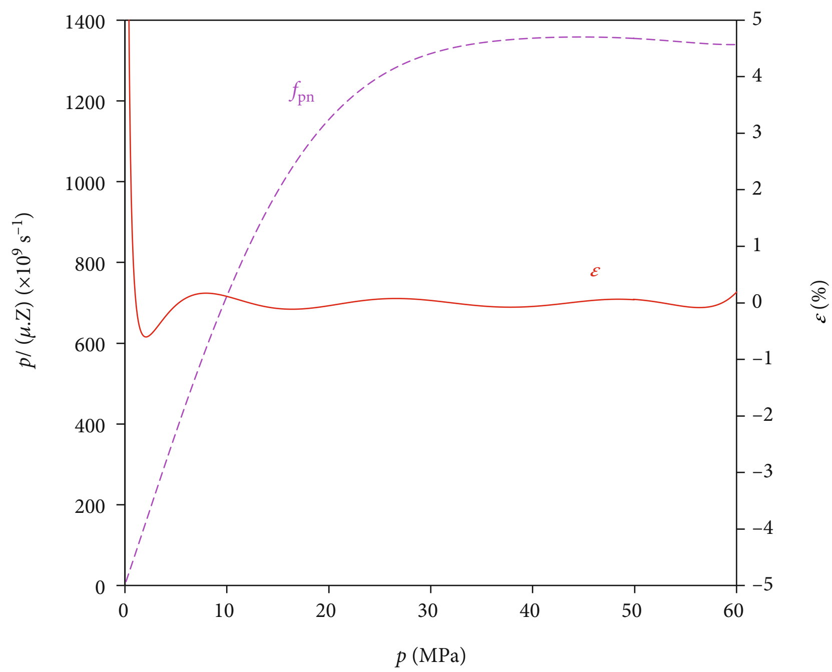

Figure 6: The relation curves of $p/(\mu Z)$ and ε vs. p calculated by the polynomial function f_{pn} for case studies.

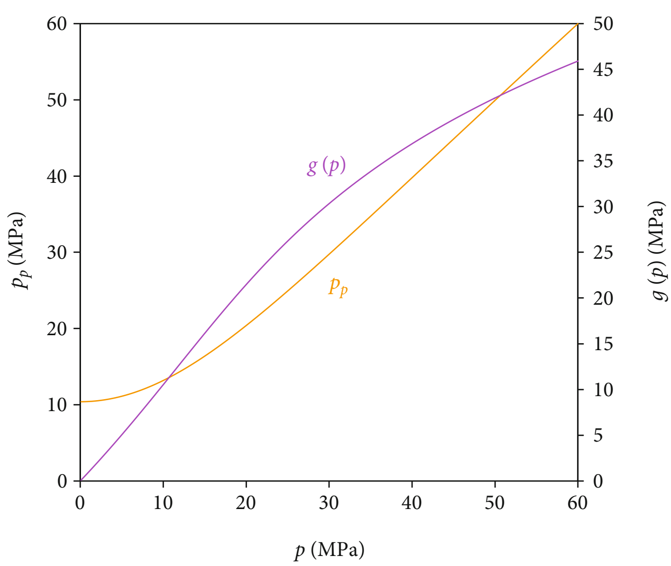

Figure 7: The relation curves of pseudopressure (p_p) and $g(p)$ vs. pressure (p) for case studies.

So, Equation (39) can be reduced to

$$g(p_{\text{ave}}) = -\frac{p_{\text{i}}}{Z_{\text{i}}} \cdot \frac{1}{G} \cdot G_{\text{p}} + \frac{p_{\text{i}}}{Z_{\text{i}}}, \tag{41}$$

$$m_{\text{smb}} = \frac{p_{\text{i}}}{Z_{\text{i}}} \cdot \frac{1}{G}. \tag{42}$$

Equation (41), termed "static material balance equation" (SMBE), reflects the relationship between cumulative gas production and average reservoir pressure. The ARP profile can be inferred from the GPPF $f_{\text{pn}}(p)$ and production data, and the gas reserves can be estimated by the negative slope (m_{smb}) of the $g(p_{\text{ave}})$ vs. G_{p} curve.

2.4. Main Steps for ARP Estimation. The pressure-rate correlations during BDF (including the dynamic material balance equation) are derived rigorously from the gas flow theory for the closed gas reservoirs, and the theoretical bases for the developed methodology for the determination of ARP and gas reserves are also explained in the earlier article. Note that the shape factor [19, 33] can be introduced into Equations (21) and (29) to delineate the

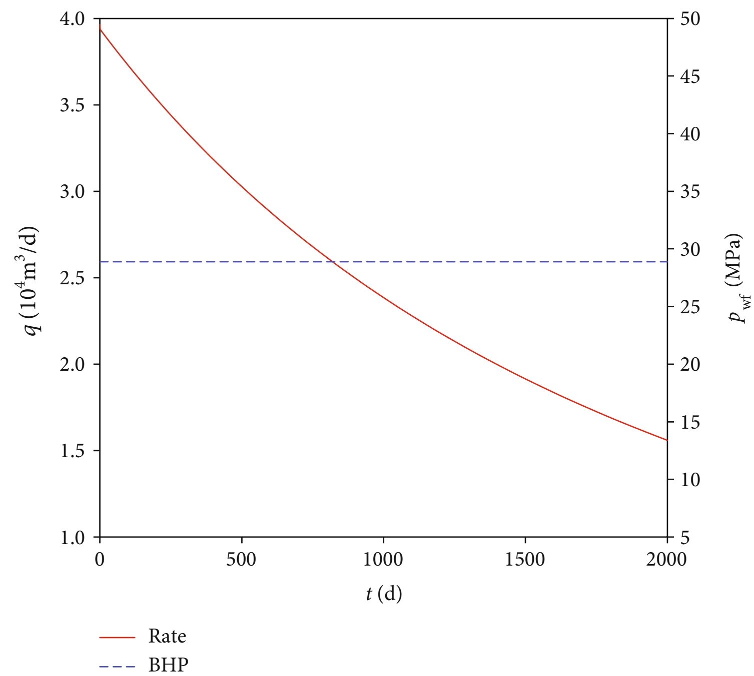

FIGURE 8: Production history of the gas well producing at a constant BHP.

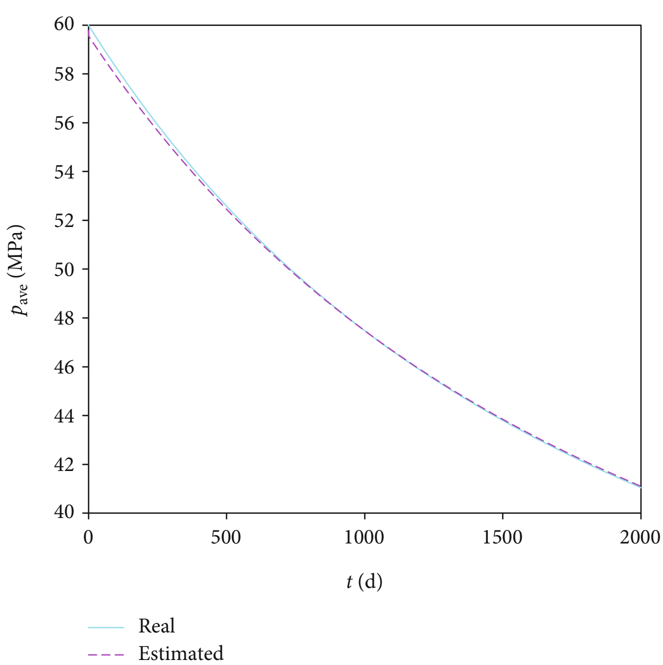

FIGURE 9: The real and estimated profiles of average reservoir pressure for the constant BHP gas well.

gas well performance in noncircular reservoirs, and it will not be discussed in detail here.

The main steps of the explicit approach presented in the paper are described below. Firstly, the property parameters of the reservoir and natural gas are needed such as reservoir temperature, initial pressure, compressibility (C_w, C_ϕ), and pseudocritical temperature and pressure of gas. So, the gas properties (such as viscosity, Z-factor, and compressibility C_g) can be determined by corresponding correlations, and the behavior of the elastic effect function $g(p)$ with pressure can also be described by Equation (40). Secondly, it is easy to establish the relation of $f(p)$ or $p/(\mu \cdot Z)$ to p, and one can use the polynomial function $f_{pn}(p)$ to replace $f(p)$; then, $F(p)$, as the primitive function of $f(p)$, can be determined. Thirdly, gas production data are necessary such as rate, BHP, and cumulative gas production. Then, we need to choose a reference point in BDF to estimate the profile of ARP by Equation (35). Lastly, gas reserves can be inferred

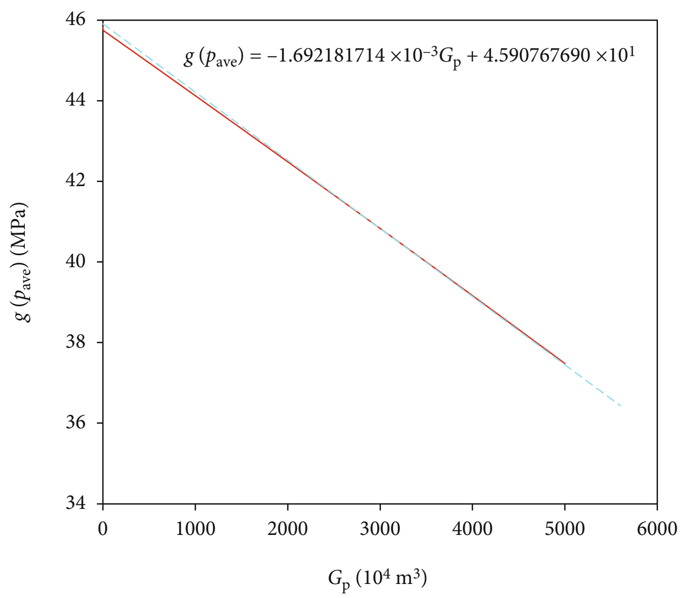

FIGURE 10: The relation of $g(p_{ave})$ to G_p for the gas well producing at a constant BHP.

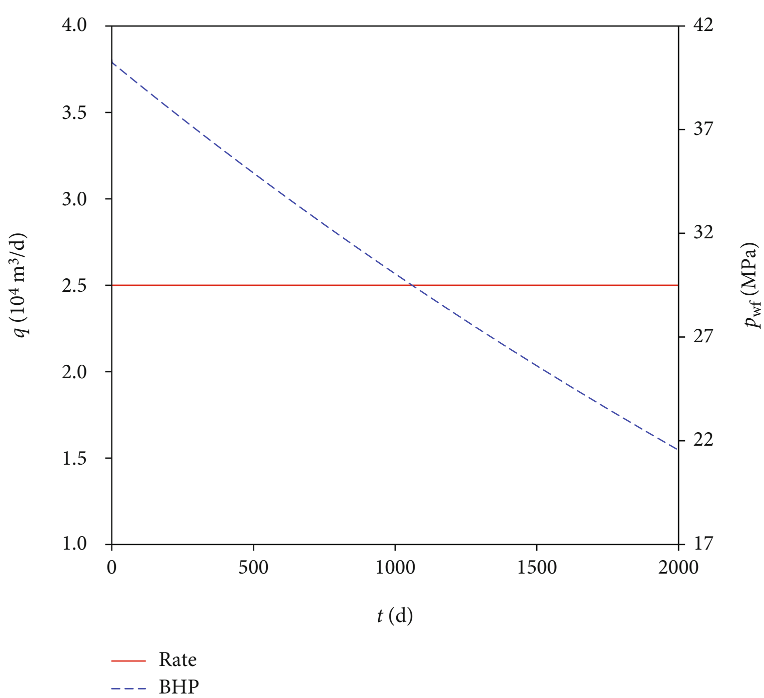

FIGURE 11: Production history of the gas well producing at a constant production rate.

from the $g(p_{ave})$ vs. G_p straight line according to Equation (41) by which in turn the obtained reserves are available to determine the formation pressure profile. The key procedures are summarized in Figure 1.

3. Model Validation

The reservoir simulator is used to generate production data including production rate, BHP, and cumulative gas production when production constraints of gas well are constant BHP, constant rate, and variable BHP/variable rate, respectively. The radial grid number is $300 \times 120 \times 1$. The initial formation pressure p_i is 60 MPa, the original formation temperature T_i is 100°C, and the initial porosity ϕ_i is 0.19. The radial permeability K_r and K_θ are both 8 mD, while the vertical permeability K_z equals 0.8 mD. The initial irreducible water saturation S_{wci} is 0.21, and the gas reservoir top depth is set to 2996 m with a reservoir thickness of 8 m. The equilibrium initialization indicates that $V_{pi} = 967\,412$ m^3, $G = 271\,300\,553$ m^3, and $p_i/Z_i = 45.908$ MPa. The compressibilities of

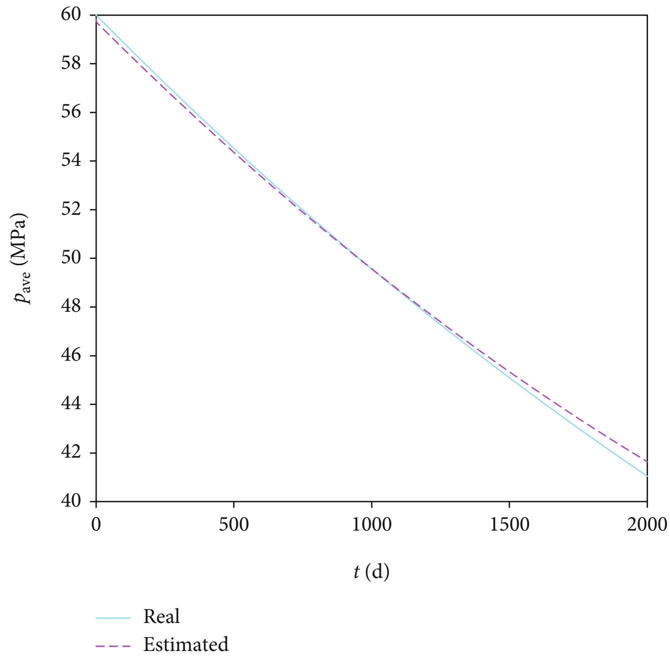

FIGURE 12: The real and estimated profiles of average reservoir pressure for the gas well producing at a constant production rate.

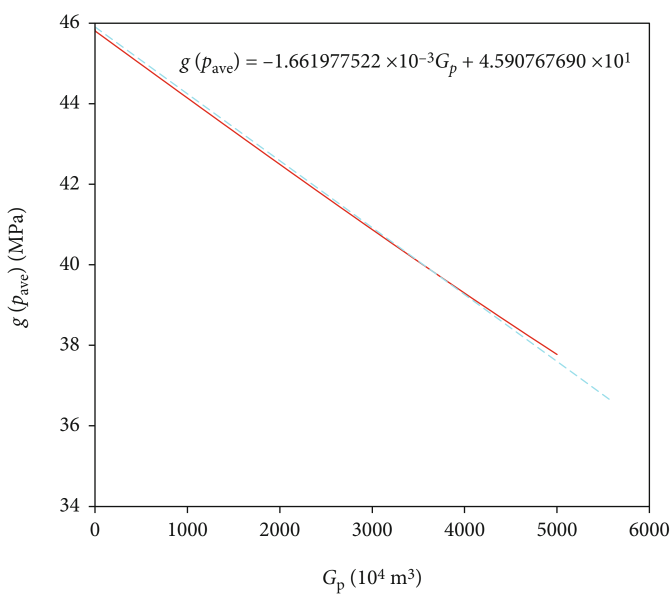

FIGURE 13: The relation of $g(p_{ave})$ to G_p for the gas well producing at a constant production rate.

rock and irreducible water are set by empirical formulas [42, 43], and other gas reservoir parameters are shown in Table 1.

The viscosity correlations proposed by Londono et al. [44, 45] are used to obtain the viscosity data of natural gas, and the Hall-Yarborough method [46] is used to calculate the deviation factor Z and the gas compressibility C_g. The Z-factor and gas compressibility curves generated by the Hall-Yarborough correlations are displayed in Figures 2 and 3, respectively, where C_{pr} in Figure 3 represents the pseudoreduced compressibility [47–50] given by

$$C_g = C_{pr} p_{pc}^{-1}. \tag{43}$$

The curves of gas formation volume factor B_g vs. pressure p and viscosity μ vs. p are shown in Figure 4. Figure 5 reveals the changes in $p/(\mu Z)$ and μZ with pressure p which also indicates that using pressure squared

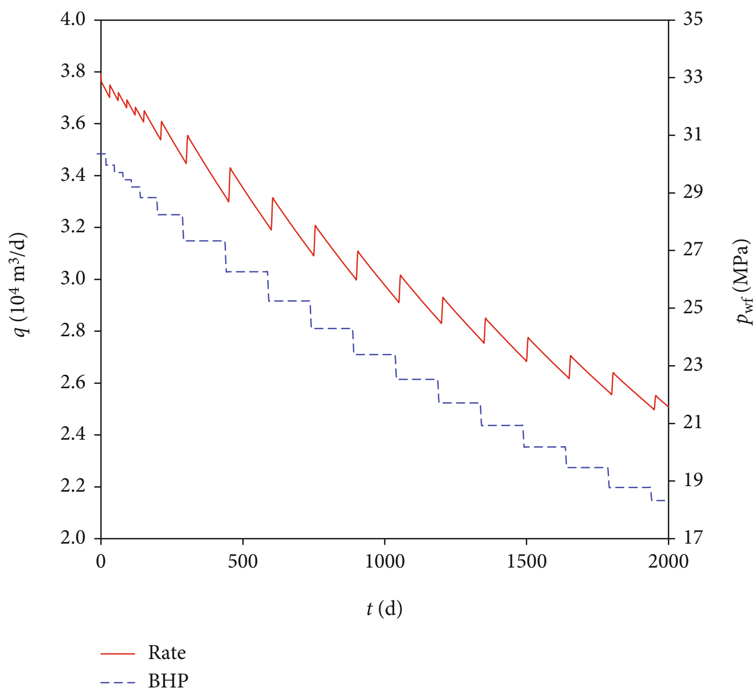

Figure 14: Production history of the gas well under variable BHP and variable rate conditions.

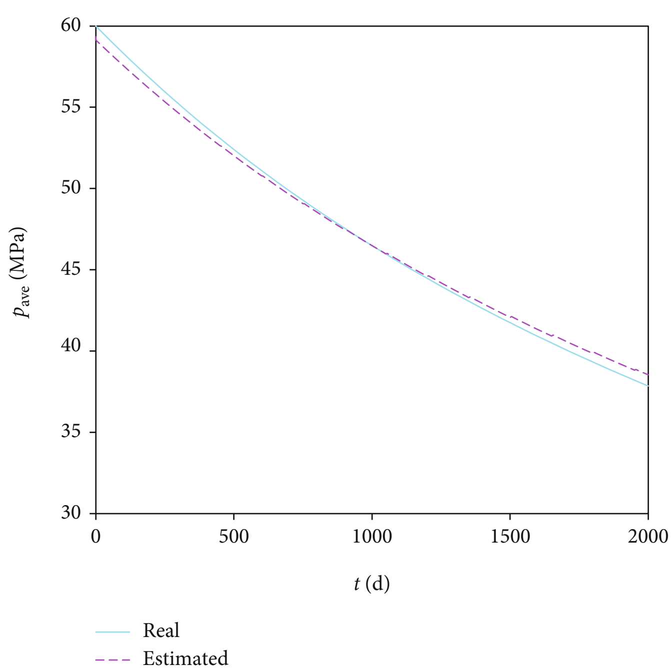

Figure 15: The real and estimated profiles of average reservoir pressure for the gas well under variable BHP and variable production rate conditions.

approximation may cause large errors, and $\mu Z/p$ is only approximately a constant when the pressure is high.

Figure 6 displays the integrand in pseudopressure obtained by Equation (45) and its error range, where ε is defined as

$$\varepsilon = \frac{f_{pn} - f}{f} \times 100\%, \tag{44}$$

$$\begin{aligned} f_{pn}(p) \approx\ & 2.863218 \times 10^{-7} p^6 - 6.009013 \\ & \times 10^{-5} p^5 + 4.746580 \times 10^{-3} p^4 \\ & - 1.595755 \times 10^{-1} p^3 + 8.873368 \\ & \times 10^{-1} p^2 + 7.437974 \times 10^{1} p + 2.473877. \end{aligned} \tag{45}$$

It can be seen from Figure 6 that the polynomial function, f_{pn}, can accurately represent the values of $f(p)$ or p

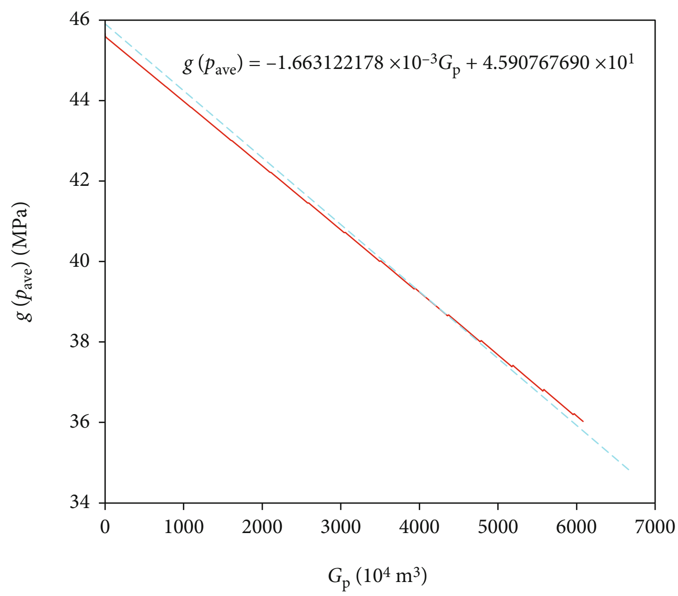

FIGURE 16: The relation of $g(p_{ave})$ to G_p for the gas well under variable BHP and variable production rate conditions.

$/(\mu Z)$ in the range of 0.7~60 MPa, and the error is no more than 1%. Figure 7 reveals the relation of the pseudo-pressure $p_p(p)$ to pressure p and that of the elastic effect function $g(p)$ to pressure p. All of them have the same dimension as the pressure.

3.1. Constant BHP Production System. The gas well's BHP is set to 28.884 MPa to simulate the 2000-day production process of the gas reservoir, in which the number of time steps adopted is 564. The production rate profile is shown in Figure 8.

Taking the production time of the 1000th day as the reference point t_k, we can get $p_k = 47.477$ MPa and $q_k = 2.385 \times 10^4$ m^3/d. Based on the rate and flowing pressure data, the ARP profile can be inferred by Equation (35), as shown in Figure 9.

After the gas reservoir pressures are inferred, the correlation between the elastic effect function $g(p_{ave})$ and the cumulative gas production G_p can be determined by the $g(p)$ vs. p curve. As shown in Figure 10, the SMBE shows m_{smb} of 1.692×10^{-3} MPa/(10^4 m^3), and the gas reserves are determined to be 2.713×10^8 m^3, only with an error of -0.003%. If another known measured pressure in the BDF stage is selected as the reference point, the result will change slightly but will not cause a large error. It is recommended to use midsection data in the evaluation period as reference points.

3.2. Constant Rate Production System. The production constraint of the gas well is set at a constant production rate, i.e., $q = 2.500 \times 10^4$ m^3/d, with other conditions unchanged. The simulated BHP profile is shown in Figure 11.

Taking the production time of the 1000th day as the reference point t_k, then p_k is 49.570 MPa with $p_{wf,k}$ of

TABLE 2: Reservoir and gas properties for the field case.

Property parameters	Property values
ϕ_i	1.354×10^{-1}
S_{wci}	2.618×10^{-1}
h	114.148 m
p_i	96.527 MPa
T_i	366.483 K
T_{sc}	293.150 K
p_{sc}	1.013×10^5 Pa
M	19.268 g/mol
T_{pc}	200 K
p_{pc}	4.600 MPa
ρ_{sc}	0.803 kg/m^3
Z_{sc}	0.998
Z_i	1.747
C_ϕ	8.702×10^{-4} MPa^{-1}
C_w	5.802×10^{-4} MPa^{-1}
μ_i	4.752×10^{-2} cp
μ_{sc}	1.055×10^{-2} cp
C_{gi}	3.478×10^{-3} MPa^{-1}
C_{ti}	3.590×10^{-3} MPa^{-1}
B_{gi}	2.299×10^{-3} m^3/m^3

30.053 MPa. Based on the production data, the ARP profile estimated by Equation (35) is illustrated in Figure 12.

Figure 12 shows that the difference between the estimated p_{ave} and the actual ARP in the later simulation stage

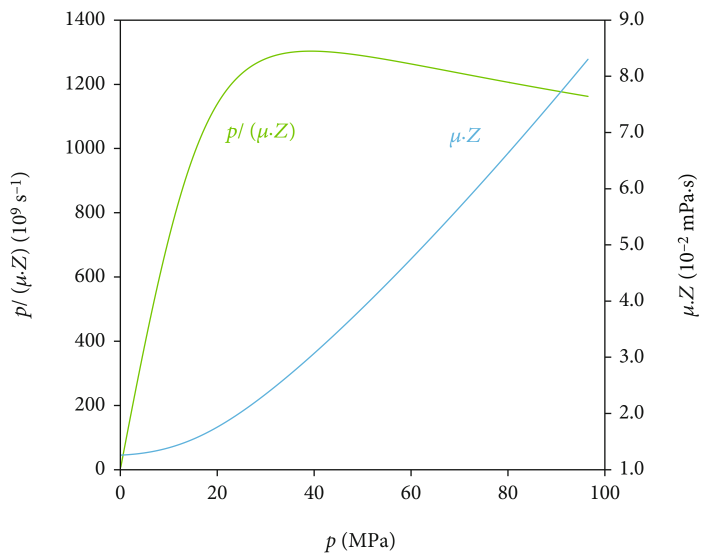

Figure 17: The relation curves of $p/(\mu Z)$ and μZ vs. pressure (p) for the field case.

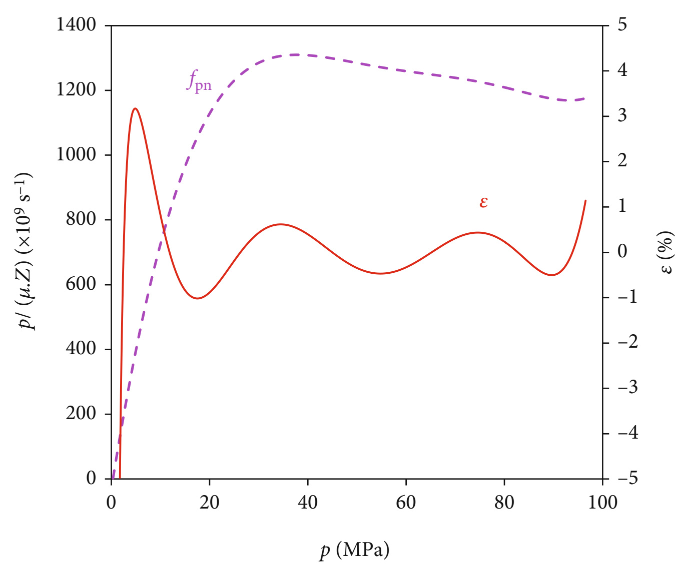

Figure 18: The relation curves of $p/(\mu Z)$ and ε vs. p calculated by the polynomial function f_{pn} for the field case.

gradually increases due to the slow variations of b in the dynamic material balance equation. The change becomes relatively obvious with a relatively long production time. The static material balance correlation obtained from the estimated ARP is exhibited in Figure 13, indicating $m_{\text{smb}} = 1.662 \times 10^{-3}\,\text{MPa}/(10^4\,\text{m}^3)$ and that subsequently the gas reserves are $2.762 \times 10^8\,\text{m}^3$ with an error of merely 1.814%. The results demonstrate that the proposed method for estimation of average reservoir pressure and gas in place is also applicable to production systems at a constant rate.

3.3. Variable BHP and Variable Rate Production Systems. We keep the gas reservoir parameters and natural gas properties unchanged and periodically change the BHP and production rate of the gas well to simulate the complex variable BHP/variable rate production schedules. The production history of the gas well is shown in Figure 14.

Similarly, taking the production time of the 1000th day as the reference point, we obtain $p_k = 46.490\,\text{MPa}$, $q_k = 2.977 \times 10^4\,\text{m}^3/\text{d}$, and $p_{\text{wf},k} = 23.290\,\text{MPa}$. Then, the estimated profile of ARP and the static material balance curve are displayed in Figures 15 and 16, respectively.

The slope of the $g(p_{\text{ave}})$ vs. G_{p} curve, m_{smb}, is $1.663 \times 10^{-3}\,\text{MPa}/(10^4\,\text{m}^3)$; hence, the gas in place is estimated to be $2.760 \times 10^8\,\text{m}^3$ with an error of 1.744%. It can be observed from Figures 15 and 16 that the value gap of b between the initial stage and the reference point is slightly larger than that between the reference point and medium late stage due to fluctuations of gas well production, changes in BHP, and long production period. Selecting the

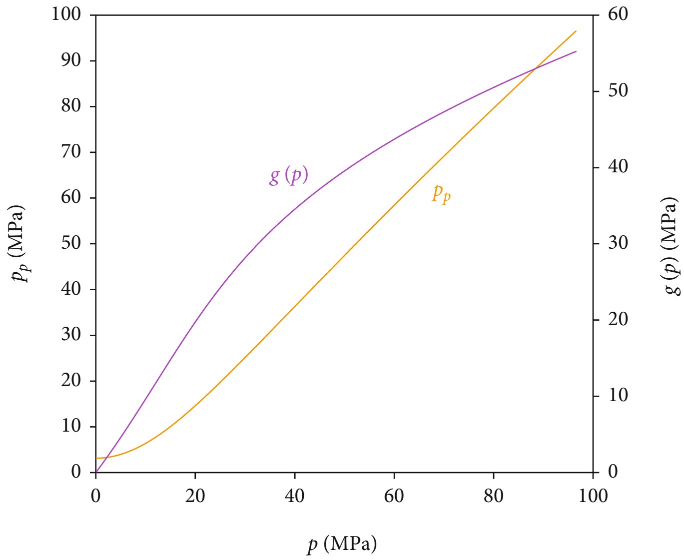

FIGURE 19: The relation curves of pseudopressure (p_p) and $g(p)$ vs. pressure (p) for the field case.

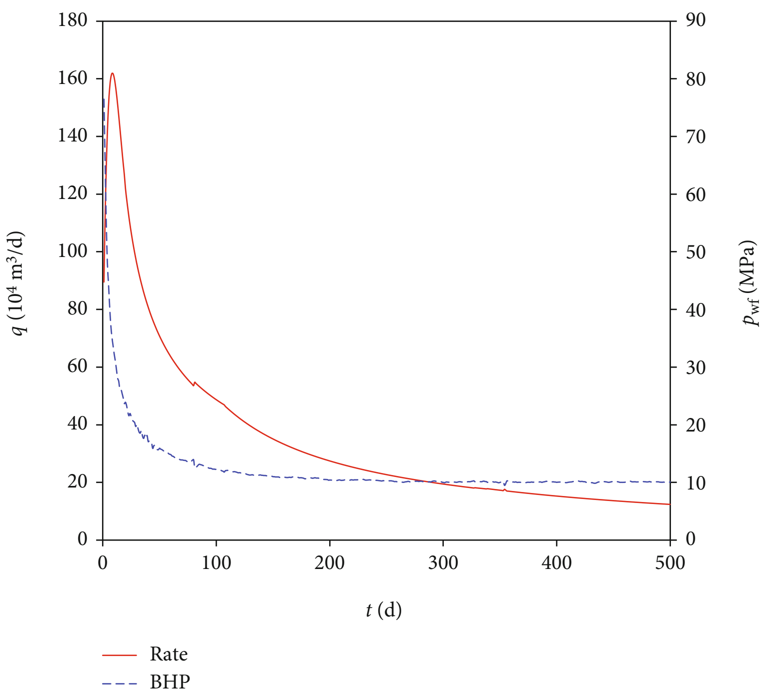

FIGURE 20: Production history of the gas well H-58.

midsection data in the evaluation period as reference points may alleviate the fluctuations of b.

The above three numerical examples have effectively proved the validity of the explicit method for estimating the average reservoir pressure and gas reserves based on the GPPF in the paper. Only one measured formation pressure is needed to give an understanding of the pressure drop history and gas in place based on the proposed method, which is widely applicable to various production systems as long as the BDF condition is satisfied. It is worth mentioning that the estimation error of the ARP and reserves may increase slightly if the measured pressure data are available merely at the beginning or end of production or if the formation pressure at the reference point is inferred by the initial pressure, production rate, and BHP data.

3.4. Field Case. The field case (well H-58) [51] is derived from Ibrahim et al. [52] who employed the superposition normalized pseudotime correlation to smooth field data and more accurately determine gas reserves. This gas well is from a tight gas reservoir with high pressure. The gas in place calculated from their normalized pseudotime plotting

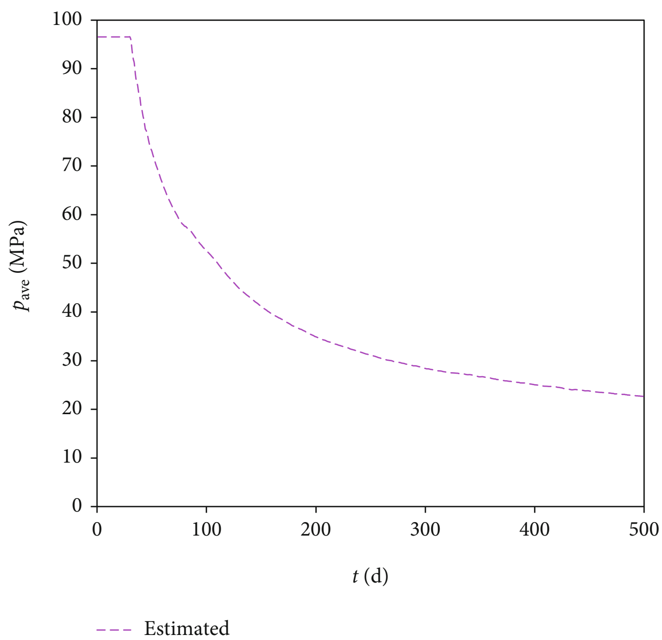

FIGURE 21: The estimated profile of average reservoir pressure for the gas well H-58.

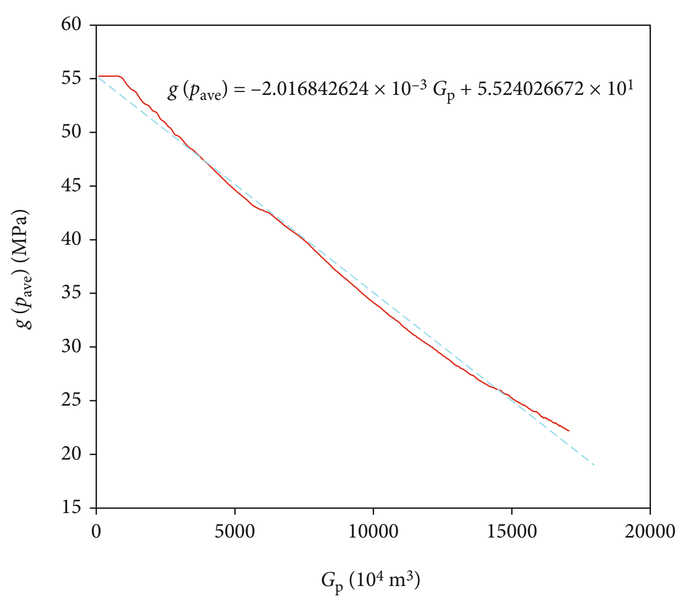

FIGURE 22: The relation of $g(p_{ave})$ to G_p for the gas well H-58.

function gives 9.8 Bcf. Table 2 shows the reservoir properties and fluid parameters. The formation temperature T_i is 93.333°C, the original formation pressure p_i is equal to 96.527 MPa, and p_i/Z_i is 55.240 MPa.

Figure 17 illustrates the variations of $f(p)$ and μZ with pressure p which indicates a possible large error caused by the pressure squared approximation and that $\mu Z/p$ is only approximately constant at relatively high pressure. Figure 18 shows the integrand in pseudopressure calculated by the GPPF (f_{pn}) and its error where the expression of f_{pn} fitted by the least square method is given by

$$\begin{aligned} f_{pn}(p) \approx{} & 2.364940 \times 10^{-8} p^6 - 6.219404 \\ & \times 10^{-6} p^5 + 4.933695 \times 10^{-4} p^4 \\ & + 1.569904 \times 10^{-3} p^3 - 2.069461 p^2 \\ & + 9.564624 \times 10^1 p - 2.970716 \times 10^1. \end{aligned} \tag{46}$$

It can be seen from Figure 18 that the polynomial function,

f_{pn}, can accurately represent the solution of $f(p) = p/(\mu Z)$ within the pressure range of 2.3~96.5 MPa, and errors of most of the results do not exceed 1%. Figure 19 shows the changes in $p_p(p)$ and $g(p)$ with p. The production rate and bottom hole flowing pressure data of well H-58 are exhibited in Figure 20.

Taking the production time of the 250th day as the reference point, it is inferred that $p_k = 31.089$ MPa, $q_k = 22.724 \times 10^4$ m^3/d, and $p_{wf,k} = 10.217$ MPa. The estimated formation pressure profile is displayed in Figure 21. It can be observed that the initial production is not stable, and the estimated formation pressure does not drop, which may be caused by the mismatches of b between the initial points and the reference point. Part of the estimated pressure data during that period should be removed when one determines the gas reserves. Figure 22 shows the static material balance relationship of the gas well H-58 where the slope of the $g(p_{ave})$ vs. G_p relationship curve m_{smb} equals 2.017×10^{-3} MPa/(10^4 m^3), and subsequently, the gas reserves are estimated to be 2.739×10^8 m^3 which is close to the estimate of Ibrahim et al. [52] (9.8 Bcf = 2.775×10^8 m^3).

4. Conclusions

The correlation between pressure and flow rate during BDF is derived in this paper using the theory of gas flow through porous media and the superposition principle. Based on the dynamic material balance equation (DMBE), a novel explicit method for estimating the ARP is proposed by using the gas property polynomial to approximate the nonlinear function, $f = p/\mu Z$. The conclusions are drawn as follows:

(i) The differences among many definitions of pseudopressure for the linearization of the governing equation for gas flow are the integral calculation with respect to f or $p/\mu Z$. In view of the limitations of pressure and pressure squared, high-order polynomials can be employed to describe the nonlinear characteristics of the integrand f

(ii) Knowledge of the formation pressure at a certain point in the BDF stage can infer the ARP profile based on the DMBE and the GPPF. This method avoids the iteration of pseudotime and is widely applicable to various production constraints such as constant BHP, constant rate, and variable BHP/variable rate as long as the BDF condition holds true (that is, b can be approximated as a constant). It is recommended to use the data in the middle evaluation period as the reference point

(iii) Once the ARP is estimated, the gas reserves can also be determined by the SMBE. This method is simple and efficient and can be in conjunction with other methods to achieve mutual verification

(iv) The presented method takes into account the compressibilities of natural gas, rock pores, and irreducible water and is suitable for both abnormally pressured gas reservoirs and normal pressure gas reservoirs

(v) The presented method assumes the BDF condition after the transient flow for the gas well in a closed reservoir. The explicit PDA (including RTA and PTA) methods dispensing with pseudotime iteration and repeated curve fitting, however, remain investigated for determination of ARP for unconventional gas reservoirs subject to long periods of transient flow conditions

Nomenclature

$\vec{v}_g$:	Velocity vector (m^3/s)
μ:	Gas viscosity (Pa·s)
K:	Effective permeability (m^2)
p:	Pressure (Pa)
ϕ:	Porosity (fraction)
ϕ_i:	Initial porosity (fraction)
C_ϕ:	Rock compressibility (Pa^{-1})
p_i:	Initial reservoir pressure (Pa)
V_p:	Pore volume (m^3)
V_{pi}:	Initial pore volume (m^3)
V_w:	Irreducible water volume (m^3)
V_{wi}:	Initial irreducible water volume (m^3)
C_w:	Water compressibility (Pa^{-1})
S_{wc}:	Irreducible water saturation (fraction)
S_{wci}:	Initial saturation of irreducible water (fraction)
ρ_g:	Gas density (kg/m^3)
M:	Gas molar mass (kg/mol)
Z:	Z-factor (compressibility factor) (fraction)
R:	Molar gas constant (8.3144598) (J/(mol·k))
T:	Temperature (K)
C_g:	Gas compressibility (Pa^{-1})
$\dot{q}_g$:	Source or sink term (kg/(m^3·s))
t:	Time (s)
C_t:	Total compressibility (system compressibility) considering elastic effects of gas, rock, and irreducible water (Pa^{-1})
μ_i:	Initial gas viscosity (Pa·s)
C_{ti}:	Initial total compressibility (Pa^{-1})
p_p:	Pseudopressure (Pa)
t_a:	Pseudotime (s)
$f(p)$:	Integrand in the pseudopressure definition (s^{-1})
$F(p)$:	Original function of $f(p)$ (Pa/s)
C_0:	Approximate constant of $\mu \cdot Z$ (Pa·s)
C_1:	Approximate constant of $\mu \cdot Z/p$ (s)
$C_0{}'$, $C_1{}'$:	Arbitrary constant (Pa/s)
α_t:	Conversion factor of dimensionless time (fraction)
α_p:	Conversion factor of dimensionless pressure (fraction)
r:	Distance from some point to the well center (m)
r_e:	Distance from the boundary to the well center (m)
r_w:	Wellbore radius (m)

B_{gi}: Initial gas formation volume factor (m^3/m^3)
h: Effective thickness (m)
r_D: Dimensionless distance (dimensionless)
t_D: Dimensionless time (dimensionless)
p_D: Dimensionless pressure (dimensionless)
λ_n: nth root of the equation $J_1(r_{eD}\lambda)Y_1(\lambda) - Y_1(r_{eD}\lambda)J_1(\lambda) = 0$ (dimensionless)
J_1: First-order Bessel function of the first kind (—)
J_0: Zero-order Bessel function of the first kind (—)
Y_1: First-order Bessel function of the second kind (Neumann function) (—)
Y_0: Zero-order Bessel function of the second kind (—)
r_{eD}: Dimensionless distance corresponding to the boundary r_e (dimensionless)
p_{p_i}: Pseudopressure corresponding to p_i (Pa)
$t_{a,i}$: Pseudotime at the end of the ith production stage (s)
q_i: Production rate of the ith production stage (m^3/s)
$p_{p_{wf}}$: Pseudopressure corresponding to BHP (Pa)
t_{ca}: Material-balance pseudotime (s)
A: Gas reservoir area (m^2)
p_{ave}: Average reservoir pressure (ARP) (Pa)
$p_{wf,k}$: BHP corresponding to the kth time (t_k) (Pa)
q_k: Production rate corresponding to t_k (m^3/s)
p_k: Average formation pressure corresponding to t_k (Pa)
f_{pn}: Polynomial to delineate the gas property function $p/(\mu Z)$ (s^{-1})
G: Gas in place or gas reserves (m^3)
B_g: Gas formation volume factor (m^3/m^3)
ΔV_p: Decremental volume of rock pores (m^3)
ΔV_w: Incremental volume of irreducible water (m^3)
G_p: Cumulative gas production (m^3)
Z_i: Original gas compressibility factor (fraction)
T_i: Original formation temperature (K)
Z_{sc}: Z-factor under standard conditions (fraction)
p_{sc}: Pressure under standard conditions (1.01325×10^5) (Pa)
T_{sc}: Temperature under standard conditions (293.15) (K)
C_{pr}: Pseudoreduced compressibility (dimensionless)
p_{pc}: Pseudocritical pressure (Pa)
T_{pc}: Pseudocritical temperature (K)
p_{pr}: Pseudoreduced pressure (dimensionless).

Data Availability

No data were used to support this study.

Conflicts of Interest

The authors declare that they have no known competing financial interests or personal relationships that could have appeared to influence the work reported in this paper.

Acknowledgments

This study has been supported by the Department of Middle East E&P and Department of Asia-Pacific E&P, Research Institute of Petroleum Exploration and Development, PetroChina. This research was funded by the National Science and Technology Major Project of China (Grant Nos. 2017ZX05030003 and 2016ZX05015002). The APC was funded by the Research Institute of Petroleum Exploration and Development, PetroChina.

References

[1] A. U. Chaudhry, *Gas Well Testing Handbook*, Gulf Professional Publishing, Burlington, MA, 2003.

[2] J. P. Spivey and W. J. Lee, *Applied Well Test Interpretation*, Society of Petroleum Engineers, Richardson, TX, 2013.

[3] D. T. Lu and X. Y. Kong, "By use of the integral of pressure distribution to calculate the average reservoir pressure," *Acta Petrolei Sinica*, vol. 14, no. 1, pp. 81–91, 1993.

[4] P. C. Li, X. Y. Kong, and D. T. Lu, "Calculating average gas reservoir pressure by integrating pseudo-pressure distribution," *Natural Gas Industry*, vol. 20, no. 3, pp. 67–69, 2000.

[5] D. R. Horner, "Pressure build-up in wells," in *Paper WPC-4135 Presented at the 3rd World Petroleum Congress*, The Hague, the Netherlands, 1951.

[6] C. C. Miller, A. B. Dyes, and C. A. Hutchinson, "The estimation of permeability and reservoir pressure from bottom hole pressure build-up characteristics," *Journal of Petroleum Technology*, vol. 2, no. 4, pp. 91–104, 1950.

[7] C. S. Matthews, F. Brons, and P. Hazebroek, "A method for determination of average pressure in a bounded reservoir," *Transactions of the AIME*, vol. 201, no. 1, pp. 182–191, 1954.

[8] D. N. Dietz, "Determination of average reservoir pressure from build-up surveys," *Journal of Petroleum Technology*, vol. 17, no. 8, pp. 955–959, 1965.

[9] H. J. Ramey and W. M. Cobb, "A general pressure buildup theory for a well in a closed drainage area (includes associated paper 6563)," *Journal of Petroleum Technology*, vol. 23, no. 12, pp. 1493–1505, 1971.

[10] A. S. Odeh and R. Al-Hussainy, "A method for determining the static pressure of a well from buildup data," *Journal of Petroleum Technology*, vol. 23, no. 5, pp. 621–624, 1971.

[11] J. G. Hu, F. Z. Yao, and J. A. Zhao, "A simple method for determining the average reservoir pressure of gas wells," *Well Testing*, vol. 2, no. 1, pp. 45–48 & 63, 1993.

[12] X. L. Qiang, K. F. Wen, and Y. H. Hao, "A facility way to determine formation pressure of gas well," *Well Testing*, vol. 14, no. 5, pp. 11–13, 2005.

[13] W. Fuping, H. Quanhua, and Y. Haibo, "Method optimizing of using production data to calculate formational pressure of gas well," *Fault-Block Oil & Gas Field*, vol. 16, no. 1, pp. 66–68, 2009.

[14] J. J. Arps, "Analysis of decline curves," *Transactions of the AIME*, vol. 160, no. 1, pp. 228–247, 1945.

[15] M. J. Fetkovich, "Decline curve analysis using type curves," *Journal of Petroleum Technology*, vol. 32, no. 6, pp. 1065–1077, 1980.

[16] M. J. Fetkovich, M. E. Vienot, M. D. Bradley, and U. G. Kiesow, "Decline-curve analysis using type curves—case histories," *SPE Formation Evaluation*, vol. 2, no. 4, pp. 637–656, 1987.

[17] R. D. Carter, "Characteristic behavior of finite radial and linear gas flow systems-constant terminal pressure case," in *Paper SPE-9887-MS presented at the SPE/DOE Low Permeability Gas Reservoirs Symposium*, Denver, Colorado, 1981.

[18] R. D. Carter, "Type curves for finite radial and linear gas-flow systems: constant-terminal-pressure case," *Society of Petroleum Engineers Journal*, vol. 25, no. 5, pp. 719–728, 1985.

[19] T. A. Blasingame and W. J. Lee, "Variable-rate reservoir limits testing of gas wells," in *Paper SPE-17708-MS presented at the SPE Gas Technology Symposium*, Dallas, Texas, 1988.

[20] T. A. Blasingame, T. L. McCray, and W. J. Lee, "Decline curve analysis for variable pressure drop/variable flowrate systems," in *Paper SPE-21513-MS presented at the SPE Gas Technology Symposium*, Houston, Texas, 1991.

[21] J. C. Palacio and T. A. Blasingame, "Decline-curve analysis using type curves-analysis of gas well production data," in *Paper SPE-25909-MS presented at the SPE Rocky Mountain Regional/Low Permeability Reservoirs Symposium*, Denver, Colorado, 1993.

[22] R. G. Agarwal, D. C. Gardner, S. W. Kleinsteiber, and D. D. Fussell, "Analyzing well production data using combined type curve and decline curve analysis concepts," in *Paper SPE-49222-MS presented at the SPE Annual Technical Conference and Exhibition*, New Orleans, Louisiana, 1998.

[23] R. G. Agarwal, D. C. Gardner, S. W. Kleinsteiber, and D. D. Fussell, "Analyzing well production data using combined-type-curve and decline-curve analysis concepts," *SPE Reservoir Evaluation & Engineering*, vol. 2, no. 5, pp. 478–486, 1999.

[24] T. A. Blasingame, J. L. Johnston, and W. J. Lee, "Type-curve analysis using the pressure integral method," in *Paper SPE-18799-MS presented at the SPE California Regional Meeting*, Bakersfield, California, 1989.

[25] L. Mattar and R. McNeil, "The "flowing" material balance procedure," in *Paper PETSOC-95-77 presented at 46th Annual Technical Meeting of The Petroleum Society of CIM*, Banff in Alberta, 1995.

[26] L. Mattar and R. McNeil, "The "flowing" gas material balance," *Journal of Canadian Petroleum Technology*, vol. 37, no. 2, pp. 52–55, 1998.

[27] Y. Q. Yang, "Calculation of average reservoir pressure by using modified flowing material balance," *Fault-Block Oil & Gas Field*, vol. 22, no. 6, pp. 747–751, 2015.

[28] C. P. Xin, Y. K. Wang, Y. L. Xu, L. Y. Shi, and Y. H. Du, "Tight gas reservoir dynamic reserve calculation with modified flowing material balance," *Special Oil & Gas Reservoirs*, vol. 25, no. 2, pp. 95–98, 2018.

[29] L. Mattar and D. Anderson, "Dynamic material balance (oil or gas-in-place without shut-ins)," in *Paper PETSOC-2005-113 presented at the Petroleum Society's 6th Canadian International Petroleum Conference (56th Annual Technical Meeting)*, Calgary, Alberta, 2005.

[30] L. Mattar, D. Anderson, and G. Stotts, "Dynamic material balance-oil-or gas-in-place without shut-ins," *Journal of Canadian Petroleum Technology*, vol. 45, no. 11, pp. 7–10, 2006.

[31] P. Ye and H. L. F. Ayala, "A density-diffusivity approach for the unsteady state analysis of natural gas reservoirs," *Journal of Natural Gas Science and Engineering*, vol. 7, pp. 22–34, 2012.

[32] T. N. Stumpf and L. F. Ayala, "Rigorous and explicit determination of reserves and hyperbolic exponents in gas-well decline analysis," *SPE Journal*, vol. 21, no. 5, pp. 1843–1857, 2016.

[33] L. X. Zhang, C. Q. Guo, H. Jiang, G. Q. Cao, and P. Y. Chen, "Gas in place determination by material balance-quasipressure approximation condition method," *Acta Petrolei Sinica*, vol. 40, no. 3, pp. 337–349, 2019.

[34] Y. Wang and L. F. Ayala, "Explicit determination of reserves for variable-bottomhole-pressure conditions in gas rate-transient analysis," *SPE Journal*, vol. 25, no. 1, pp. 369–390, 2020.

[35] K. Jongkittinarukorn, N. Last, F. H. Escobar, and F. Srisuriyachai, "A straight-line DCA for a gas reservoir," *Journal of Petroleum Science and Engineering*, vol. 201, article 108452, 2021.

[36] J. Ansah, R. S. Knowles, and T. A. Blasingame, "A semi-analytic (p/z) rate-time relation for the analysis and prediction of gas well performance," in *Paper SPE-35268-MS presented at the SPE Mid-Continent Gas Symposium*, Amarillo, Texas, 1996.

[37] J. Ansah, R. S. Knowles, and T. A. Blasingame, "A semi-analytic (p/z) rate-time relation for the analysis and prediction of gas well performance," *SPE Reservoir Evaluation & Engineering*, vol. 3, no. 6, pp. 525–533, 2000.

[38] L. Mattar and D. M. Anderson, "A systematic and comprehensive methodology for advanced analysis of production data," in *Paper SPE-84472-MS presented at the SPE Annual Technical Conference and Exhibition*, Denver, Colorado, 2003.

[39] H. D. Sun, *Advanced Production Decline Analysis and Application*, Gulf Professional Publishing, Waltham, MA, 2015.

[40] R. E. Terry and J. B. Rogers, *Applied Petroleum Reservoir Engineering*, Pearson Education Inc, New York, 3rd Edition edition, 2015.

[41] M. Sanni, *Petroleum Engineering: Principles, Calculations, and Workflows*, American Geophysical Union and John Wiley & Sons Inc, Washington, 2019.

[42] T. L. Qin, D. Li, and Y. Q. Chen, *Practical Reservoir Engineering Methods*, Petroleum Industry Press, Beijing, 1989.

[43] Y. Q. Chen and D. Li, *Modern Petroleum Reservoir Engineering*, Petroleum Industry Press, Beijing, 2001.

[44] F. E. Londono, R. A. Archer, and T. A. Blasingame, "Simplified correlations for hydrocarbon gas viscosity and gas density-validation and correlation of behavior using a large-scale database," in *Paper SPE-75721-MS presented at the SPE Gas Technology Symposium*, Calgary, Alberta, 2002.

[45] F. E. Londono, R. A. Archer, and T. A. Blasingame, "Correlations for hydrocarbon-gas viscosity and gas density-validation and correlation of behavior using a large-scale database," *SPE Reservoir Evaluation & Engineering*, vol. 8, no. 6, pp. 561–572, 2005.

[46] K. R. Hall and L. Yarborough, "A new equation of state for Z-factor calculations," *Oil and Gas Journal*, vol. 71, no. 25, pp. 82–92, 1973.

[47] A. S. Trube, "Compressibility of natural gases," *Journal of Petroleum Technology*, vol. 9, no. 1, pp. 69–71, 1957.

[48] L. Mattar, G. S. Brar, and K. Aziz, "Compressibility of natural gases," *Journal of Canadian Petroleum Technology*, vol. 14, no. 4, pp. 77–80, 1975.

[49] J. H. Abou-Kassem, L. Mattar, and P. M. Dranchuk, "Computer calculations of compressibility of natural gas," *Journal of Canadian Petroleum Technology*, vol. 29, no. 5, pp. 105–108, 1990.

[50] S. G. Ghedan, M. S. Aljawad, and F. H. Poettmann, *Compressibility of Natural Gases*, SPE Technical Publications, 1991.

[51] L. X. Zhang, Y. Li, X. M. Song et al., "A new method for estimating gas reserves using production data and pseudovariables," *Proceedings of the International Field Exploration and Development Conference 2021. IFEDC 2021. Springer Series in Geomechanics and Geoengineering*Springer, Singapore.

[52] M. Ibrahim, R. A. Wattenbarger, and W. Helmy, "Determination of OGIP for wells in pseudosteady-state-old techniques, new approaches," in *Paper SPE-84286-MS presented at the SPE Annual Technical Conference and Exhibition*, Denver, Colorado, 2003.